Environ Fluid Mech (2010) 10:7–20
DOI 10.1007/s10652-009-9145-4

ORIGINAL ARTICLE

A comparison of three Eulerian numerical methods for fractional-order transport models

Emmanuel Hanert

Received: 12 March 2009 / Accepted: 16 July 2009 / Published online: 1 August 2009

Abstract Tracer transport in complex systems like turbulent flows or heterogeneous porous media is now more and more regarded as a non-local process that can hardly be represented by second-order diffusion models. In this work, we consider diffusion models that assume that tracer particles follow a heavy-tail Lévy distribution, which allows for large displacements. We show that such an assumption leads to a fractional-order diffusion operator in the governing equation for tracer concentration. A comparison of three Eulerian numerical methods to discretize that equation is then performed. These consist of the finite difference, finite element and spectral element methods. We suggest that non-local methods, like the spectral element method, are better suited to transport models with fractional-order diffusion operators.

Keywords Tracer transport · Fractional calculus · Lévy distributions · Spectral element method

1 Introduction

For many environmental problems, it is important to be able to describe the transport dynamics without having recourse to a direct numerical simulation of all the processes taking place in the system, which often requires excessive computational resources. For efficient and practical predictions, simpler and more manageable models should be sought in order to capture the phenomena of interest without having to calculate all the details of the complex system. Examples include moisture, pollutants and chemical components in the atmosphere; salinity and temperature in the ocean; sediments in rivers and lakes, contaminants and nutriments in heterogeneous porous media, etc.

E. Hanert (✉)
Department of Environmental Sciences and Land Use Planning, Université Catholique de Louvain, Place Croix du Sud 2/16, 1348 Louvain-la-Neuve, Belgium
e-mail: emmanuel.hanert@uclouvain.be

Dispersion processes in complex systems are generally described by a second-order advection–diffusion equation (ADE). The assumption underlying this model is that turbulent dispersion, like molecular diffusion, can be described by Fick's law, which states that particle flux is directly proportional to the spatial concentration gradient. Fick's law therefore assumes that the spatial concentration gradient is causing particles movement in a turbulent flow. This assumption is contradicted by observations that suggest that particles in a turbulent flow do not "push" each other as it is the case for Brownian motion but are rather dispersed by the velocity fluctuations. A number of studies have shown that Fickian diffusion was unsatisfactory to simulate tracer transport in environmental flows (see for instance [1,24,27,28,31]). All these studies have highlighted the dependence of the eddy viscosity on the size of the dispersion cloud. Different Lagrangian [10,12,19] and Eulerian [4] modelling approaches have been proposed to account for the observed non-Fickian dispersion patterns. The limitations of eddy diffusivity models are further discussed in a recent paper by Cushman-Roisin [8].

Despite the apparent shortcomings of the second-order diffusion operator to represent dispersion in complex systems, it is still used in the majority of today's models of environmental flows. However, a number of recent studies advocate the use of non-local and scale-dependent dispersion models to simulate the transport of tracers in complex systems. Such models are usually based on fractional-order diffusion operators (see for instance [2,7,22,30]). They have been used to model tracer transport in systems such as saturated and unsaturated soil layers [5,16,18,25], river flows [11,20] or the atmospheric boundary layer [9]. For these applications, the use of fractional temporal models is sometimes required as well [33].

Although non-local tracer transport models are now an active field of research, they are still in their infancy and many questions remain. One of them concerns the numerical methods that should be used to efficiently discretize the fractional-order diffusion operator. If such models are to be used operationally to simulate complex environmental systems, they have to achieve good accuracy at the same computational cost as traditional models. In this work, we compare three different Eulerian numerical methods: the finite difference, finite element and spectral element methods.

2 Theory

In laminar homogeneous flows, the dispersion of tracer particles is mainly driven by the mean flow velocity and by local interactions between particles that result in regular and isotropic random displacements. These random displacements constitute a Brownian motion. Since all these random fluctuations can be assumed to be independent and identically distributed, and the variance of their sum can be assumed to be finite, then de Moivre's Central Limit Theorem (CLT) indicates that the sum of all the random displacements will follow a Gaussian probability distribution function whose center moves with the fluid mean velocity. In one dimension, this probability distribution function is a solution of the following second-order ADE:

$$\frac{\partial c}{\partial t} + v\frac{\partial c}{\partial x} = K\frac{\partial^2 c}{\partial x^2}. \tag{1}$$

The concentration c can be seen as the probability distribution function of a large number of tracer particles that experience a deterministic drift of velocity v and a normal random fluctuation with standard deviation equal to $\sqrt{2Kt}$, where K is a macroscopic diffusion coefficient. Einstein [13] first made the link between the second-order ADE and Brownian

motion. It should be noted that Eq. 1 can also be obtained by using Fick's parameterization of the concentration flux.

In turbulent heterogeneous flows, particles can be transported over large distances by the fluctuations of the flow velocity. In that case, although local interactions are still possible, longer and non-local interactions should also be taken into account. In addition to that one should also allow for non-isotropic random displacements than can arise from the heterogeneous nature of the system. The resulting ensemble of random displacements, in the limit where the ensemble size tends to infinity, does not necessarily have a finite variance. The standard version of the CLT can therefore not be applied. Instead, the generalization due to Lévy–Gnedenko [17,21] can be used. That version of the theorem does not rely on the assumption that the sum of all the fluctuations has a finite variance but instead assumes that it has a power-law tail distribution decreasing as $|x|^{-\alpha-1}$ with $0 < \alpha \leq 2$. If we further assume that the probability of particle jumps to the right is $\frac{1-\beta}{2}$ and jumps to the left is $\frac{1+\beta}{2}$ with $-1 \leq \beta \leq 1$, then the sum of all these fluctuations will tend to a stable Lévy distribution with exponent α and skewness parameter β [14]. Such a distribution does not usually have an explicit expression but can be expressed in terms of its Fourier transform. If we define the Fourier and inverse Fourier transforms as:

$$F(\omega) = \mathcal{F}(f) = \int_{-\infty}^{\infty} f(x) e^{-i\omega x}\, \mathrm{d}x,$$

$$f(x) = \mathcal{F}^{-1}(F) = \frac{1}{2\pi} \int_{-\infty}^{\infty} F(\omega) e^{i\omega x}\, \mathrm{d}\omega,$$

we can then define the Lévy distribution as follows:

$$S_\alpha(\beta, \gamma, \delta; x) \equiv \begin{cases} \mathcal{F}^{-1}\left\{\exp\left(i\delta\omega - \gamma^\alpha |\omega|^\alpha \left(1 - i\beta \mathrm{sgn}(\omega) \tan\frac{\alpha\pi}{2}\right)\right)\right\} & \alpha \neq 1, \\ \mathcal{F}^{-1}\left\{\exp\left(i\delta\omega - \gamma^\alpha |\omega|^\alpha \left(1 + i\beta \mathrm{sgn}(\omega) \frac{2}{\pi} \log|\omega|\right)\right)\right\} & \alpha = 1, \end{cases} \tag{2}$$

where the real parameters $\gamma \in [0, \infty)$ and $\delta \in (-\infty, \infty)$ are called the scale and the location of the distribution. The former is a measure of the width of the distribution while the latter indicates the position of the center of the distribution. These parameters are similar to the mean (μ) and variance (σ^2) but the latter cannot be defined when $\alpha < 2$. Indeed, the heavy-tail behavior of stable distributions leads to an infinite variance and undefined mean for all $\alpha < 2$. Although Lévy distributions do not generally have an analytical expression, there are two noteworthy exceptions: (i) The Gaussian/normal distribution which corresponds to a Lévy stable distribution with exponent $\alpha = 2$ and variance $\sigma^2 = 2\gamma$ and (ii) the Cauchy distribution which is a Lévy distribution with exponent $\alpha = 1$. In these two cases, the skewness parameter β is irrelevant.

In Fig. 1, we show two Lévy distributions with exponents $\alpha = 2$ and $\alpha = 1.75$. For both cases, the other parameters have the following values: $\beta = 0$, $\gamma = 1$ and $\delta = 0$. We also show the dispersion pattern obtained when one particle is randomly displaced by fluctuations following these distributions without any deterministic drift. In both cases, the particle random displacement consists in 10^4 steps. When $\alpha = 2$, the particle motion is Brownian and is characterized by a succession of disordered displacements of similar length. When $\alpha = 1.75$, the motion is still mostly Brownian but the particle now has a non-negligible probability to jump over larger distances. As the value of α decreases, the thickness of the distribution's tails increases and hence the probability of large jumps increases as well.

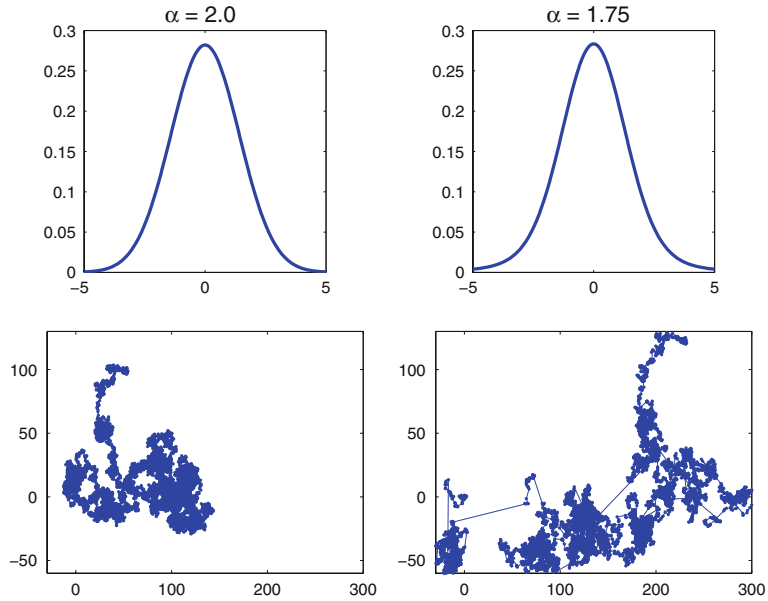

Fig. 1 *Top row*: Lévy distributions with parameters $\alpha = 2$ (*left*) and $\alpha = 1.75$ (*right*), $\beta = 0, \gamma = 1$ and $\delta = 0$. *Bottom row*: Illustration of the displacement of single particle that is randomly moved by fluctuations following these distributions. The total number of steps made by the particle is equal to 10^4. Note that the distribution's tails are thicker when $\alpha = 1.75$

Following the same approach as Benson et al. [3], we can show that the Lévy distribution is the solution of an ADE of fractional order α. Since the Fourier transform of the usual m^{th} ($m \in \mathbb{N}$) order derivative is $\mathcal{F}\{f^{(m)}\} = (i\omega)^m \mathcal{F}\{f\}$, we can define the left and right fractional-order derivatives as

$$\frac{\partial^\alpha}{\partial x^\alpha} f(x,t) = \mathcal{F}^{-1}\left\{(i\omega)^\alpha \mathcal{F}\{f\}\right\},$$
$$\frac{\partial^\alpha}{\partial(-x)^\alpha} f(x,t) = \mathcal{F}^{-1}\left\{(-i\omega)^\alpha \mathcal{F}\{f\}\right\}.$$

It can be shown (see for instance Podlubny [26] for details) that these expressions are equivalent to the Riemann–Liouville fractional derivatives defined as:

$$\frac{\partial^\alpha}{\partial x^\alpha} f(x,t) = \frac{1}{\Gamma(n-\alpha)} \frac{\partial^n}{\partial x^n} \int_{-\infty}^{x} \frac{f(y,t)}{(x-y)^{\alpha-n+1}}\, \mathrm{d}y,$$
$$\frac{\partial^\alpha}{\partial(-x)^\alpha} f(x,t) = \frac{(-1)^n}{\Gamma(n-\alpha)} \frac{\partial^n}{\partial x^n} \int_{x}^{+\infty} \frac{f(y,t)}{(y-x)^{\alpha-n+1}}\, \mathrm{d}y,$$

where $n = 1 + [\alpha]$ and $[\alpha]$ is the largest integer not greater than α, i.e., $n = 2$ for $1 < \alpha \leq 2$, and $\Gamma(.)$ is Euler's gamma function.

By using these differential operators and assuming $\alpha \neq 1$, we can define the following fractional-order ADE:

$$\frac{\partial c}{\partial t} + v\frac{\partial c}{\partial x} = K_\alpha \frac{1-\beta}{2} \frac{\partial^\alpha c}{\partial x^\alpha} + K_\alpha \frac{1+\beta}{2} \frac{\partial^\alpha c}{\partial(-x)^\alpha}. \tag{3}$$

The analytical solution of Eq. 3 can be found by taking its Fourier transform:

$$\frac{\partial C}{\partial t} + (iv\omega)C = K_\alpha \frac{1-\beta}{2}(i\omega)^\alpha C + K_\alpha \frac{1+\beta}{2}(-i\omega)^\alpha C, \tag{4}$$

where $C(\omega, t) = \mathcal{F}\{c(x,t)\}$. The solution of (4) then reads:

$$C(\omega, t) = \exp\left[-(iv\omega)t + K_\alpha \frac{1-\beta}{2}(i\omega)^\alpha t + K_\alpha \frac{1+\beta}{2}(-i\omega)^\alpha t\right]. \tag{5}$$

Using the following relations:

$$(i\omega)^\alpha = |\omega|^\alpha \left(\cos\frac{\pi\alpha}{2} + i\,\mathrm{sgn}(\omega)\sin\frac{\pi\alpha}{2}\right),$$
$$(-i\omega)^\alpha = |\omega|^\alpha \left(\cos\frac{\pi\alpha}{2} - i\,\mathrm{sgn}(\omega)\sin\frac{\pi\alpha}{2}\right),$$

we can express (5) as

$$C(\omega, t) = \exp\left[-(iv\omega)t + K_\alpha t\cos\frac{\pi\alpha}{2}|\omega|^\alpha \left(1 - i\beta\,\mathrm{sgn}(\omega)\tan\frac{\pi\alpha}{2}\right)\right],$$

and the solution of Eq. 3 thus reads

$$c(x,t) = S_\alpha\left(\beta, \left(-K_\alpha t\cos\frac{\pi\alpha}{2}\right)^{1/\alpha}, -vt; x\right).$$

It is interesting to note that the width of the distribution grows like $t^{1/\alpha}$, which clearly illustrates that fractional-order diffusion is "faster" than the usual second-order diffusion as soon as $\alpha < 2$.

3 Three Eulerian numerical methods for the fractional-order ADE

In this section, we present different numerical techniques to solve the fractional-order ADE on a finite computational domain $[0, L]$. In that case, we have to redefine the right and left fractional derivatives as follows:

$$\frac{\partial^\alpha}{\partial x^\alpha} f(x,t) = \frac{1}{\Gamma(n-\alpha)}\frac{\partial^n}{\partial x^n}\int_0^x \frac{f(y,t)}{(x-y)^{\alpha-n+1}}\,\mathrm{d}y, \tag{6}$$

$$\frac{\partial^\alpha}{\partial(-x)^\alpha} f(x,t) = \frac{(-1)^n}{\Gamma(n-\alpha)}\frac{\partial^n}{\partial x^n}\int_x^L \frac{f(y,t)}{(y-x)^{\alpha-n+1}}\,\mathrm{d}y, \tag{7}$$

to account for the restricted domain of definition of f. We consider three different Eulerian numerical methods to solve Eq. 3: the finite difference (FD), finite element (FE) and spectral element (SE) methods.

3.1 Finite difference method

A FD discretization of the fractional-order ADE can be obtained by using the so-called Grunwald fractional derivative [26] instead of the Riemann–Liouville derivatives (6) and

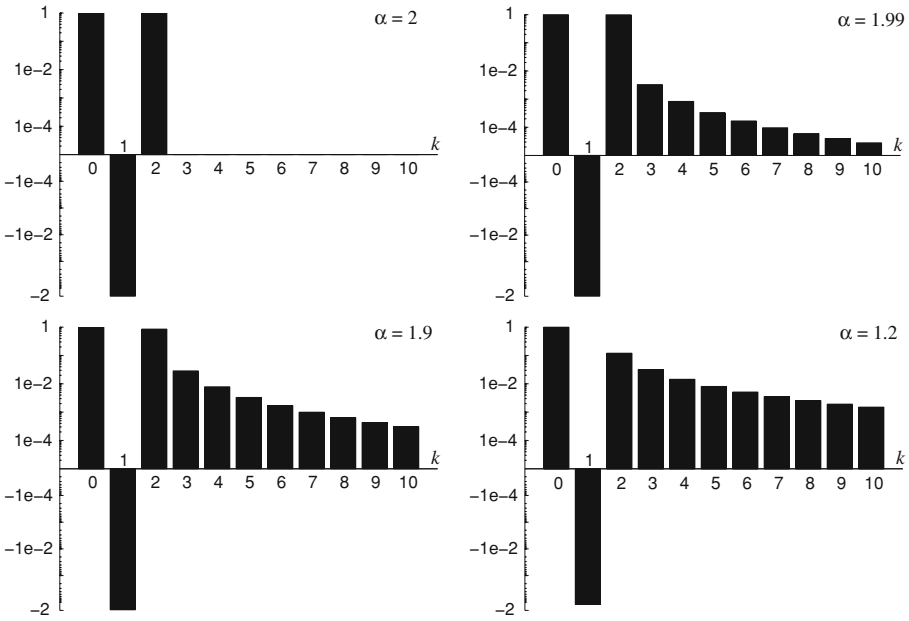

Fig. 2 First Grunwald weights w_k for different values of the exponent coefficient α and $k = 0, 1, \ldots, 10$. When $\alpha = 2$, only weights corresponding to $k = 0,\ 1$ and 2 are non-zero. As soon as $\alpha < 2$, all the other weights become positive and see their value increase as α decreases. Note that the y-axis is logarithmic and discontinuous between positive and negative values

(7). In that case, the left and right fractional derivatives are expressed as:

$$\frac{\partial^\alpha f}{\partial x^\alpha} = \lim_{M\to\infty} \frac{\sum_{k=0}^{M} w_k f(x-(k-1)\Delta x)}{\Delta x^\alpha}, \tag{8}$$

$$\frac{\partial^\alpha f}{\partial(-x)^\alpha} = \lim_{M\to\infty} \frac{\sum_{k=0}^{M} w_k f(x+(k-1)\Delta x)}{\Delta x^\alpha}, \tag{9}$$

where

$$w_k = \frac{\Gamma(k-\alpha)}{\Gamma(k+1)\Gamma(-\alpha)} \quad k = 0, 1, 2, \ldots.$$

and M is a positive integer, and $\Delta x = L/M$. The Grunwald derivative can be interpreted as a generalization to non-integer orders of the fundamental definition of derivatives in terms of quotient of differences. It can be shown that the Grunwald and Riemann-Liouville fractional-order derivatives are equivalent [26]. Note that in (8)–(9), a shifted Grunwald formula has been used for stability reasons [23].

The coefficients w_k, also called Grunwald weights, illustrate the non-locality of the fractional-order derivatives as soon as $\alpha < 2$. As shown in Fig. 2, the importance of points faraway from the point under consideration increases as α decreases. Unlike integer-order derivatives, the fractional-order differential operator is a global operator that takes into account the global behavior of the function and not just the local slope.

The expression of the Grunwald formula suggests a simple way of discretizing the fractional-order ADE in space by means of the FD method. A discrete approximation of (3) can be obtained by truncating (8)–(9) and using a finite space increment Δx. Such a FD

scheme can easily be implemented and generalized to higher dimensions. It is only first-order accurate in space but Tadjeran et al. [32] have proposed a method to improve the accuracy to second order. For instance, to solve Eq. 3 over the one-dimensional domain $[0, L]$, the following FD scheme could be used:

$$\frac{\mathrm{d}c_i}{\mathrm{d}t} + v_i \frac{c_{i+1} - c_{i-1}}{2\Delta x} = K_\alpha \frac{1-\beta}{2} \frac{\sum_{j=0}^{i} w_j c_{i-j}}{\Delta x^\alpha} + K_\alpha \frac{1+\beta}{2} \frac{\sum_{j=0}^{N-i} w_j c_{i+j}}{\Delta x^\alpha}, \quad (10)$$

where the domain has been divided in N segments of finite size $\Delta x = \frac{L}{N}$. Equation 10 has to be combined with suitable boundary conditions and discretized in time as well.

As can be seen from (10), the FD stencil used to discretize the fractional-order derivative covers the whole domain as soon as $\alpha < 2$. This could obviously be expected as fractional-order derivatives are global operators that have more similarities with integrals than with traditional derivatives. However, since the FD method usually requires a large number of nodes to obtain a precise result, the resulting increase in the computational cost can be important. In 1D, the number of operations required to compute the fractional-order derivative at a given node will be about $N/3$ times larger than the number of operations required to compute a second-order derivative. Moreover, the use of an implicit time integration scheme seems totally prohibitive as it would require to solve a full-matrix system of equations.

3.2 Finite element method

The FE method has first been applied by Fix and Roop [15] and Roop [29] to the fractional-order ADE. Unlike the FD method, the FE method does not discretize the differential operators but rather approximates the exact solution by a linear combination of basis functions ϕ_i, which are usually piecewise polynomials defined on a partition of the computational domain. The solution of (3) is thus expressed as:

$$c(x,t) \approx c^h(x,t) = \sum_{j=1}^{N} c_j(t)\phi_j(x), \quad (11)$$

where the superscript h denotes the discrete solution and the c_j's are unknown coefficients.

Before deriving the discrete equations that will allow us to compute the expansion coefficients, we shall first rewrite the fractional derivative as follows:

$$\begin{aligned}
&\frac{1-\beta}{2}\frac{\partial^\alpha c}{\partial x^\alpha} + \frac{1+\beta}{2}\frac{\partial^\alpha c}{\partial(-x)^\alpha} \\
&= \frac{\partial^n}{\partial x^n}\left[\frac{1-\beta}{2\Gamma(n-\alpha)}\int_0^x \frac{c(y,t)}{(x-y)^{\alpha-n+1}}\,\mathrm{d}y + \frac{1+\beta}{2\Gamma(n-\alpha)}\int_x^L \frac{c(y,t)}{(y-x)^{\alpha-n+1}}\,\mathrm{d}y\right] \\
&\equiv \frac{\partial^n}{\partial x^n} G_{\alpha\beta}(x,c).
\end{aligned}$$

That allows us to express the fractional derivative of c as the integer-order derivative of a space-averaging function $G_{\alpha\beta}$, which could also be expressed in terms of the convolution of $c(x,t)$ with $x^{n-\alpha-1}$. For most environmental systems, $1 < \alpha \leq 2$ and n is thus equal to 2. In that case and provided that we are able to compute $G_{\alpha\beta}$, the discrete equations can be derived

by using exactly the same standard Galerkin formulation as for the second-order ADE:

$$\int_0^L \frac{\partial c^h}{\partial t}\phi_i \,\mathrm{d}x + \int_0^L v\frac{\partial c^h}{\partial x}\phi_i \,\mathrm{d}x = K_\alpha \int_0^L \frac{\partial^2 G_{\alpha\beta}(x,c^h)}{\partial x^2}\phi_i \,\mathrm{d}x,$$
$$= -K_\alpha \int_0^L \frac{\partial G_{\alpha\beta}(x,c^h)}{\partial x}\frac{\partial \phi_i}{\partial x}\,\mathrm{d}x + \left[K_\alpha \frac{\partial G_{\alpha\beta}(x,c^h)}{\partial x}\phi_i\right]_0^L,$$

for $i = 1, \ldots, N$. By replacing c^h by the expansion in (11), we obtain the following set of N discrete equations:

$$\sum_{j=1}^N \left(\int_0^L \phi_i\phi_j \,\mathrm{d}x\right)\frac{\mathrm{d}c_j}{\mathrm{d}t} + \sum_{j=1}^N \left(\int_0^L v\phi_i\frac{\partial\phi_j}{\partial x}\,\mathrm{d}x\right)c_j$$
$$= \sum_{j=1}^N \underbrace{\left(-K_\alpha \int_0^L \frac{\partial\phi_i}{\partial x}\frac{\partial G_{\alpha\beta}(x,\phi_j)}{\partial x}\,\mathrm{d}x\right)}_{\equiv \mathrm{D}_{ij}} c_j, \tag{12}$$

where we have assumed, for simplicity, that the non-local diffusive flux $K_\alpha \frac{\partial}{\partial x}G_{\alpha\beta}(x,c^h)$ is vanishing on the boundaries.

Since ϕ_j is usually a low-order polynomial, its fractional derivative can be computed analytically (see Appendix for more details). Numerical calculations are also possible provided that the singularity at x is handled carefully. In Fig. 3, we show a piecewise linear basis function, the corresponding space-averaging function $G_{\alpha\beta}$ and the fractional derivative of order $\alpha - 1$, i.e., $\frac{\partial G_{\alpha\beta}(x,\phi_j)}{\partial x}$, for different values of α. It can be seen that the global space-averaging effect increases as α decreases. The decentering effect of the skewness parameter β is also illustrated. In this case, $G_{\alpha\beta}$ would have been symmetric for $\beta = 0$.

Like the FD method, the FE method results in a full diffusion matrix as the fractional-order derivative of a basis function is no more a local-support function. As a result, the computational cost of the numerical model is expected to substantially increase when going from second-order to fractional-order diffusion. Moreover, the calculation of the integrals involving the fractional-order derivative of a basis function might be costly. In that respect, linear basis functions are particularly interesting as their first derivative is constant. The diffusion term can thus be expressed as follows:

$$\mathrm{D}_{ij} = -K_\alpha \frac{\partial\phi_i}{\partial x}\Big|_{[x_{i-1},x_i]} \int_{x_{i-1}}^{x_i} \frac{\partial G_{\alpha\beta}(x,\phi_j)}{\partial x}\,\mathrm{d}x - K_\alpha \frac{\partial\phi_i}{\partial x}\Big|_{[x_i,x_{i+1}]} \int_{x_i}^{x_{i+1}} \frac{\partial G_{\alpha\beta}(x,\phi_j)}{\partial x}\,\mathrm{d}x$$
$$= -\frac{K_\alpha}{x_i - x_{i-1}}\left[G_{\alpha\beta}(x,\phi_j)\right]_{x_{i-1}}^{x_i} + \frac{K_\alpha}{x_{i+1} - x_i}\left[G_{\alpha\beta}(x,\phi_j)\right]_{x_i}^{x_{i+1}},$$

where we have used the fact that ϕ_i is linear and only defined on $[x_{i-1}, x_i]$ and $[x_i, x_{i+1}]$ (See Fig. 3a). Regarding conservation, the use of a Galerkin formulation and the integration by parts of the diffusion term guarantees that mass is going to be conserved globally.

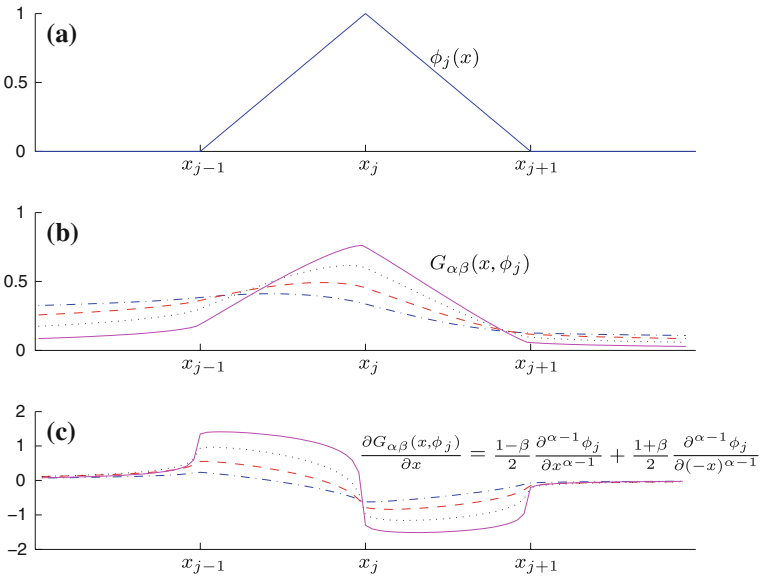

Fig. 3 Example of **(a)** a linear FE basis function ϕ_j, **(b)** the corresponding space-averaging function $G_{\alpha\beta}(x,\phi_j)$, and **(c)** the fractional derivative of ϕ_j for $\alpha = 1.2$ (.-), 1.4 (--), 1.6 (..), 1.8 (−) and $\beta = 0.5$. Note that although ϕ_j is a local-support function, its fractional derivative is not

3.3 Spectral element method

The main disadvantage of the FD and FE methods is that they both result in full diffusion matrices that could render the computational code inefficient. These methods thus require quite more operations to solve the fractional-order ADE than to solve the second-order ADE. This issue is related to the fact the both the FD and (standard low-order) FE methods are local methods that usually update one degree of freedom (dof) by using only a small number of neighboring dof's. As a result, the FD and FE methods require a large number of dof's to provide an accurate solution but are well-suited to local (i.e., integer-order) differential operators as they result in sparse system matrices. However, when applied to non-local differential operators, such numerical methods could become inefficient.

Therefore a non-local numerical method, like the SE method, might be better suited to solve Eq. 3. That method is quite similar to the FE method and also approximates the exact solution c with a discrete solution c^h defined by Eq. 4. The main difference is that the basis functions ϕ_j are now high order functions defined over the whole computational domain. Sines and cosines are typically used for periodic problems while Chebyshev or Legendre functions are used for non-periodic ones (see for instance Boyd [6] for more details). With the SE method, each dof directly depends on all the dof's defining the solution. Such methods are thus of order N, where N is the number of dof's, and the convergence rate is exponential. As a result, to obtain a given level of accuracy, the SE method requires a much smaller number of dof's than the FD and FE methods. Moreover, as the SE method always requires the calculation of integrals of complex functions over the entire computational domain, the solution of a fractional-order ADE is not expected to be substantially more expensive. To our knowledge, the SE method has never been used to solve the fractional-order ADE.

If Chebyshev basis functions and a Galerkin formulation are used, the resulting set of discrete equations is similar to (12) with the exception that (i) ϕ_i is a Chebyshev polynomial of degree i and (ii) $\mathrm{d}x$ should be multiplied by the weight $w(x) = (1-(2x/L-1)^2)^{-1/2}$ in all the integrals in order to make use of the orthogonality property of Chebyshev polynomials. In that case, the discrete equations read:

$$\sum_{j=1}^{N}\left(\int_0^L \phi_i\phi_j w(x)\,\mathrm{d}x\right)\frac{\mathrm{d}c_j}{\mathrm{d}t}+\sum_{j=1}^{N}\left(\int_0^L v\phi_i\frac{\partial\phi_j}{\partial x}w(x)\,\mathrm{d}x\right)c_j = \sum_{j=1}^{N}\underbrace{\left(K_\alpha\int_0^L \phi_i\frac{\partial^2 G_{\alpha\beta}(x,\phi_j)}{\partial x^2}w(x)\,\mathrm{d}x\right)}_{\equiv \mathrm{D}_{ij}}c_j,$$

for $i = 1,\ldots,N$. It should be noted that the diffusion term has not been integrated by parts. This is mainly because the diffusive flux $\phi_i w\frac{\partial G_{\alpha\beta}(x,c^h)}{\partial x}$ does not vanish on the boundaries of the domain since ϕ_i is a global function that is generally not equal to zero on the boundary. As a result (and unlike with the FE method), the flux term has to be computed even when Dirichlet boundary conditions are imposed, which makes it rather cumbersome.

As the SE methods requires less dof's to obtain an accurate solution, there will be less evaluations of $G_{\alpha\beta}(x,\phi_j)$ and less integrals to compute. Moreover, since Chebyshev functions are polynomials of increasing order, their fractional-order derivative can be computed analytically. Figure 4 shows a fourth order Chebyshev basis function, the corresponding space-averaged function $G_{\alpha\beta}$ and the fractional derivative for different values of α.

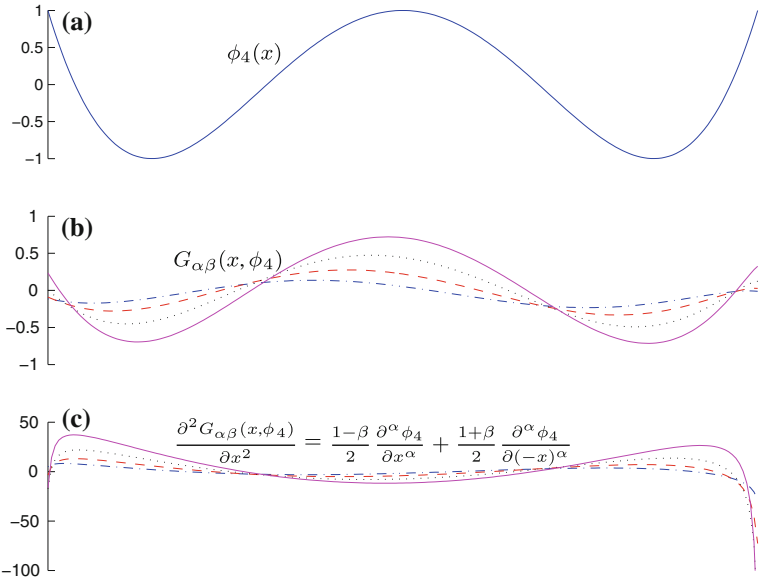

Fig. 4 Same as Fig. 3 but for a fourth-order Chebyshev polynomial. In this case, both the basis function ϕ_4 and its fractional derivative are global functions

4 Numerical example

In this section, we compare the three numerical discretizations of the fractional-order ADE introduced in the previous section. In order to assess the efficiency and accuracy of the three methods, we consider a one-dimensional benchmark problem introduced by Tadjeran et al. [32]. The problem consists in finding $c(x,t)$ such that

$$\frac{\partial c(x,t)}{\partial t} = d(x)\frac{\partial^{1.8} c(x,t)}{\partial x^{1.8}} + q(x,t) \quad \text{for } x \in [0,1] \text{ and } t > 0, \tag{13}$$

with $d(x) = \Gamma(2.2)x^{2.8}/6$, $q(x,t) = -(1+x)e^{-t}x^3$, $c(x,0) = x^3$, $c(0,t) = 0$ and $c(1,t) = e^{-t}$. In that case, the exact solution of (13) reads:

$$c(x,t) = e^{-t}x^3.$$

Equation 13 has been discretized with FD, FE and SE schemes and solved until $t = 1$. At the end of the simulation, the numerical solutions have been compared with the exact solution.

Figure 5 shows the rate of convergence of the three methods. For the FE and SE schemes, the relative error has been computed in the L_2 norm. For the FD scheme, a root mean square error has been computed. The integrals defining the FE and SE diffusion matrices have been computed numerically by means of Gauss and Gauss–Laguerre quadrature rules, respectively. As expected, the convergence rates for FD, FE and SE schemes are linear, quadratic and exponential, respectively. As mentioned previously, the linear convergence rate of the FD scheme can be increased to quadratic by using the approach proposed by Tadjeran et al. [32]. Since all the schemes result in a full diffusion matrix, the computational cost per dof is similar for the three schemes. It therefore appears that the SE scheme is the most efficient since it requires much less dof's to achieve the same accuracy. For instance, to achieve a 0.1% relative error, the FD, FE and SE schemes require about 80, 30 and 5 dof's, respectively.

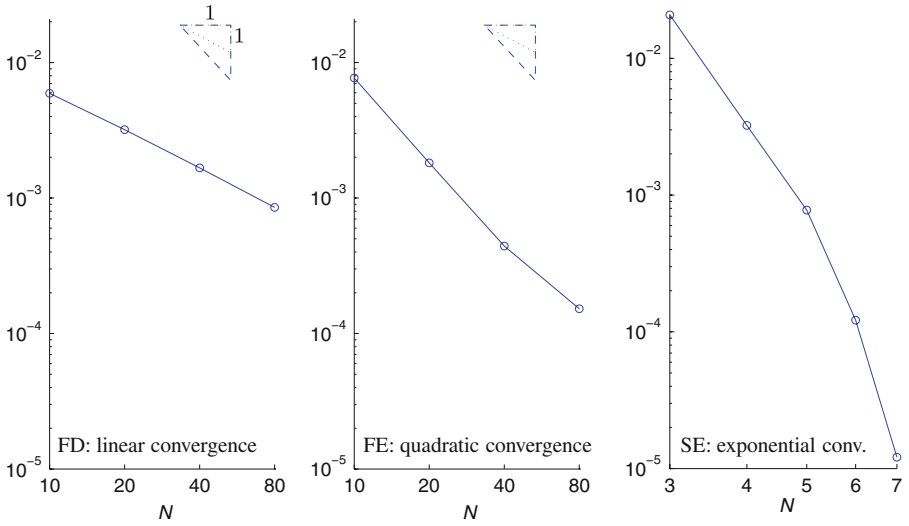

Fig. 5 Convergence analysis of the FD, FE and SE methods for Tadjeran et al.'s [32] test case. Note that approximatively 80, 30 and 5 dof's are needed for the FD, FE and SE schemes, respectively, to achieve an error level of 10^{-3}

5 Conclusion

Just as the Gaussian distribution is a special case of a Lévy distribution, second-order transport models are just a special case of fractional-order transport models. Such models allow the representation of a much larger array of processes, ranging from local molecular diffusion to non-local diffusion in complex heterogeneous systems. The non-local nature of fractional-order transport models requires a specific numerical treatment as traditional methods like the FD and FE methods are not designed to efficiently discretize non-local spatial differential operators.

Such operators are non-local in the sense that they can be expressed in terms of the integral of the solution over the entire computational domain. They are therefore better suited to non-local numerical methods, like the SE method, which naturally take the global behavior of the solution into account. The computational cost of the method does not significantly increase when moving from an integer-order to a fractional-order transport model. In addition to being more efficient than the FD and FE methods, the SE method also achieves a higher rate of convergence.

Further work will be required to design an optimal SE scheme for fractional-order transport models. For instance, the efficiency of the SE method could be further improved by deriving basis functions that would diagonalize the diffusion matrix, i.e., basis functions that are eigenfunctions of the fractional-order diffusion operator. In addition to that model parameters estimation and mathematical properties like stability, positivity, and uniqueness of the solution will have to be rigorously assessed before using such a numerical scheme for realistic environmental problems.

Appendix: analytical results

In this section, we present some analytical results useful for calculating the fractional derivatives of FE and SE basis functions. Since both sets of basis functions are polynomials, we can assume that ϕ_j has the following expression:

$$\phi_j(x) = \sum_{k=0}^{m} c_k x^k.$$

The left Riemann–Liouville derivative of ϕ_j then reads:

$$\frac{\mathrm{d}^\alpha \phi_j}{\mathrm{d}x^\alpha} = \sum_{k=0}^{m} c_k \frac{\mathrm{d}^\alpha x^k}{\mathrm{d}x^\alpha} = \frac{1}{\Gamma(n-\alpha)} \sum_{k=0}^{m} c_k \frac{\mathrm{d}^n}{\mathrm{d}x^n} \int_0^x \frac{y^k}{(x-y)^{\alpha-n+1}}\,\mathrm{d}y, \tag{14}$$

where n is such that $n-1 < \alpha \leq n$. The expression of the right Riemann–Liouville derivative is similar to (14). The integrals of the powers in (14) can be computed analytically by using the following primitives:

$$\int \frac{y^0}{(x-y)^{\alpha-n+1}}\,\mathrm{d}y = -\frac{(x-y)^{n-\alpha}}{n-\alpha}$$

$$\int \frac{y^1}{(x-y)^{\alpha-n+1}}\,\mathrm{d}y = \frac{(x-y)^{n+1-\alpha}}{n+1-\alpha} - \frac{x(x-y)^{n-\alpha}}{n-\alpha}$$

$$\int \frac{y^2}{(x-y)^{\alpha-n+1}}\,\mathrm{d}y = -\frac{(x-y)^{n+2-\alpha}}{n+2-\alpha} + \frac{2x(x-y)^{n+1-\alpha}}{n+1-\alpha} - \frac{x^2(x-y)^{n-\alpha}}{n-\alpha}$$

$$\vdots \quad = \quad \vdots$$

$$\int \frac{y^k}{(x-y)^{\alpha-n+1}}\,\mathrm{d}y = \sum_{i=0}^{k}(-1)^{i+1}\binom{k}{i}\frac{x^{k-i}(x-y)^{n+i-\alpha}}{n+i-\alpha}.$$

As an example, let us consider the FE basis function represented in Fig. 3. It can be expressed as:

$$\phi_j(x) = \begin{cases} 0 & x < x_j \text{ or } x \geq x_{j+1}, \\ \frac{x-x_{j-1}}{x_j-x_{j-1}} & x_{j-1} \leq x < x_j, \\ \frac{x_{j+1}-x}{x_{j+1}-x_j} & x_j \leq x < x_{j+1}. \end{cases}$$

For that basis function, the left Riemann–Liouville derivative reads:

$$\frac{\mathrm{d}^\alpha \phi_j(x)}{\mathrm{d}x^\alpha} = \frac{1}{\Gamma(n-\alpha)} \times \frac{\mathrm{d}^n}{\mathrm{d}x^n} \begin{cases} 0 & x < x_{j-1}, \\ \frac{1}{x_j-x_{j-1}}\frac{(x-x_{j-1})^{n-\alpha+1}}{(n-\alpha)(n-\alpha+1)} & x_{j-1} \leq x < x_j, \\ \frac{1}{x_j-x_{j-1}}\left[(x-x_j)^{n-\alpha}\left(\frac{x-x_j}{n+1-\alpha}-\frac{x-x_{j-1}}{n-\alpha}\right)+\frac{(x-x_{j-1})^{n-\alpha+1}}{(n-\alpha)(n-\alpha+1)}\right] & \\ \quad +\frac{1}{x_{j+1}-x_j}\left[(x-x_j)^{n-\alpha}\left(\frac{x-x_j}{n+1-\alpha}-\frac{x-x_{j+1}}{n-\alpha}\right)\right] & x_j \leq x < x_{j+1}, \\ \frac{1}{x_j-x_{j-1}}\left[(x-x_j)^{n-\alpha}\left(\frac{x-x_j}{n+1-\alpha}-\frac{x-x_{j-1}}{n-\alpha}\right)+\frac{(x-x_{j-1})^{n-\alpha+1}}{(n-\alpha)(n-\alpha+1)}\right] & \\ \quad +\frac{1}{x_{j+1}-x_j}\left[(x-x_j)^{n-\alpha}\left(\frac{x-x_j}{n+1-\alpha}-\frac{x-x_{j+1}}{n-\alpha}\right)+\frac{(x-x_{j+1})^{n-\alpha+1}}{(n-\alpha)(n-\alpha+1)}\right] & x \geq x_{j+1}. \end{cases}$$

It can be seen that for $1 < \alpha \leq 2, n = 2$ and the expression above diverges at the mesh nodes. However, in the FE formulation (12), only derivatives of order $\alpha - 1$ are considered. In that case, $n = 1$ and the fractional derivative of a basis function remains bounded.

References

1. Batchelor GK (1950) The application of the similarity theory of turbulence to atmospheric diffusion. Quart J R Meteorol Soc 76:133–146
2. Benson DA, Wheatcraft SW, Meerschaert MM (2000) Application of a fractional advection-dispersion equation. Water Resour Res 36:1403–1412
3. Benson DA, Wheatcraft SW, Meerschaert MM (2000) The fractional-order governing equation of levy motion. Water Resour Res 36:1413–1423
4. Berkowicz R, Prahm L (1979) Generalization of K theory for turbulent diffusion. Part 1: spectral diffusivity concept. J Appl Meteorol 18:266–272
5. Berkowitz B, Cortis A, Dentz M, Scher H (2006) Modelling non-Fickian transport in geological formations as a continuous time random walk. Rev Geophys 44(RG2003):3
6. Boyd JP (2001) Chebyshev and Fourier spectral methods, 2nd edn. Dover Publications, New York
7. Chaves AS (1998) A fractional diffusion equation to describe Lévy flights. Phys Lett A 239:13–16
8. Cushman-Roisin B (2008) Beyond eddy diffusivity: an alternative model for turbulent dispersion. Environ Fluid Mech 8:543–549
9. Cushman-Roisin B, Jenkins AD (2006) On a non-local parameterization for shear turbulence and the uniqueness of its solutions. Boundary-Layer Meteorol 118:69–82
10. Davies RE (1983) Oceanic property transport, Lagrangian particle statistics, and their prediction. J Mar Res 41:163–194
11. Deng ZQ, Bengtson L, Singh VP (2006) Parameter estimation for fractional dispersion model for rivers. Environ Fluid Mech 6:451–475

12. Durbin PA (1980) A stochastic model of two-particle dispersion and concentration fluctuations in homogeneous turbulence. J Fluid Mech 100:279–302
13. Einstein A (1905) Uber die von der molekularkinetischen Theorie der Wärme geforderte Bewegung von in ruhenden Flüssigkeiten suspendierten Teilchen. Annalen der Physik 17:549–560
14. Feller W (1971) An introduction to probability theory and its applications, vol II. Wiley, New York
15. Fix GJ, Roop JP (2004) Least square finite-element solution of a fractional order two-point boundary value problem. Comput Math Appl 48:1017–1033
16. Frippiat CC, Holeyman AE (2008) A comparative review of upscaling methods for solute transport in heterogenenous porous media. J Hydrol 362:150–176
17. Gnedenko B, Kolmogorov A (1954) Limit distributions for sums of independent random variables. Addison-Wesley, Cambridge, MA
18. Huang G, Huang Q, Zhan H (2006) Evidence of one-dimensional scale-dependent fractional advection-dispersion. J Contam Hydrol 85:53–71
19. Jenkins AD (1985) Simulation of turbulent dispersion using a simple random model of the flow field. Appl Math Model 9:239–245
20. Kim S, Kavvas ML (2006) Generalized Fick's law and fractional ADE for pollution transport in a river: detailed derivation. J Hydrol Eng 11(1):80–83
21. Lévy P (1954) Théorie de l'Addition des Variables Aléatoires. Gauthier-Villars, Paris
22. Meerschaert MM, Benson DA, Bäumer B (1999) Multidimensional advection and fractional dispersion. Phys Lett A 59:5026–5028
23. Meerschaert MM, Tadjeran C (2004) Finite difference approximations for fractional advection-diffusion flow equations. J Comput Appl Math 172:65–77
24. Okubo A (1971) Oceanic diffusion diagrams. Deep Sea Res 18:789–802
25. Pachepsky Y, Timlin D, Rawls W (2003) Generalized Richards' equation to simulate water transport in unsaturated soils. J Hydrol 272:3–13
26. Podlubny I (1999) Fractional differential equations: mathematics in science and engineering, vol 198. Academic Press, New York
27. Richardson LF (1926) Atmospheric diffusion shown on a distance-neighbour graph. Proc R Soc Lond 110:709–737
28. Richardson LF, Stommel H (1948) Note on eddy diffusion in the sea. J Meteorol 5:238–240
29. Roop JP (2006) Computational aspects of FEM approximation of fractional advection dispersion equations on bounded domains in $\mathbb{R}^2$. J Comput Appl Math 193:243–268
30. Schumer R, Benson DA, Meerschaert MM, Wheatcraft JW (2001) Eulerian derivation of the fractional advection-dispersion equation. J Contam Hydrol 48:69–88
31. Stommel H (1949) Horizontal diffusion due to oceanic turbulence. J Mar Res 8:199–225
32. Tadjeran C, Meerschaert MM, Scheffler H-P (2006) A second-order accurate numerical approximation for the fractional diffusion equation. J Comput Phys 213:205–213
33. Zhang Y, Benson DA, Reeves DM (2009) Time and space nonlocalities underlying fractional-derivative models: Distinction and literature review of field applications. Adv Water Resour 32(4):561–581